Serine Hydroxymethyltransferase: Role of Glu75 and Evidence that Serine Is Cleaved by a Retroaldol Mechanism†

Doletha M. E. Szebenyi,‡ Faik N. Musayev,§ Martino L. di Salvo,|| Martin K. Safo,§ and Verne Schirch*,||

MacCHESS at Cornell High Energy Synchrotron Source, Cornell University, Ithaca, New York 14853, and Institute for Structural Biology and Drug Discovery and Department of Biochemistry, Virginia Commonwealth University, Richmond, Virginia 23219

Received January 29, 2004; Revised Manuscript Received March 29, 2004

ABSTRACT: Serine hydroxymethyltransferase (SHMT) catalyzes the reversible interconversion of serine and glycine with tetrahydrofolate serving as the one-carbon carrier. SHMT also catalyzes the folate-independent retroaldol cleavage of allothreonine and 3-phenylserine and the irreversible conversion of 5,10-methenyltetrahydrofolate to 5-formyltetrahydrofolate. Studies of wild-type and site mutants of SHMT have failed to clearly establish the mechanism of this enzyme. The cleavage of 3-hydroxy amino acids to glycine and an aldehyde occurs by a retroaldol mechanism. However, the folate-dependent cleavage of serine can be described by either the same retroaldol mechanism with formaldehyde as an enzyme-bound intermediate or by a nucleophilic displacement mechanism in which N5 of tetrahydrofolate displaces the C3 hydroxyl of serine, forming a covalent intermediate. Glu75 of SHMT is clearly involved in the reaction mechanism; it is within hydrogen bonding distance of the hydroxyl group of serine and the formyl group of 5-formyltetrahydrofolate in complexes of these species with SHMT. This residue was changed to Leu and Gln, and the structures, kinetics, and spectral properties of the site mutants were determined. Neither mutation significantly changed the structure of SHMT, the spectral properties of its complexes, or the kinetics of the retroaldol cleavage of allothreonine and 3-phenylserine. However, both mutations blocked the folate-dependent serine-to-glycine reaction and the conversion of methenyltetrahydrofolate to 5-formyltetrahydrofolate. These results clearly indicate that interaction of Glu75 with folate is required for folate-dependent reactions catalyzed by SHMT. Moreover, we can now propose a promising modification to the retroaldol mechanism for serine cleavage. As the first step, N5 of tetrahydrofolate makes a nucleophilic attack on C3 of serine, breaking the C2−C3 bond to form N5-hydroxymethylene-tetrahydrofolate and an enzyme-bound glycine anion. The transient formation of formaldehyde as an intermediate is possible, but not required. This mechanism explains the greatly enhanced rate of serine cleavage in the presence of folate, and avoids some serious difficulties presented by the nucleophilic displacement mechanism involving breakage of the C3−OH bond.

Serine hydroxymethyltransferase (SHMT)[1] catalyzes the reversible interconversion of serine and glycine with the hydroxymethyl group of serine (C3) being transferred to H_4-PteGlu$_n$ to form CH_2-H_4PteGlu$_n$ (*1*). This reaction serves as the major source of one-carbon groups required for the biosynthesis of purines, thymidylate, methionine, and many neurotransmitters. SHMT contains tightly bound PLP, and it is the interplay of H_4PteGlu$_n$ with PLP that is of great interest in terms of both the catalytic mechanism and nutritional studies that show a link between these two vitamins.

After the discovery of SHMT activity, the enzyme was named serine aldolase, because it was conceived that the mechanism of the enzyme involved a retroaldol cleavage of serine to form formaldehyde and glycine (Figure 1a). In a second step, the bound formaldehyde was thought to condense with H_4PteGlu$_n$ to form CH_2-H_4PteGlu$_n$ (Figure 1b). This proposed mechanism was strengthened when it was discovered that SHMT catalyzes, without the need for H_4-PteGlu, the rapid retroaldol cleavage of threonine and β-phenylserine to glycine with acetaldehyde and benzaldehyde, respectively (*2*, *3*).

SHMT has also been shown to catalyze the conversion of 5,10-CH^+-H_4PteGlu$_n$ to 5-CHO-H_4PteGlu$_n$ (Figure 1c) (*4*); in this case, the 1-C group is at the oxidation level of formate

† This study was supported in part by U.S. Public Health Service Grant DK56648 to V.S. and by NIH NCRR Division Grant RR-01646 to MacCHESS. Some experimental work was carried out at CHESS, which is supported by NSF Grant DMR97-13424.

* To whom correspondence should be addressed: Department of Biochemistry, 1101 E. Marshall St., Box 614, Virginia Commonwealth University, Richmond, VA 23298. E-mail: Schirch@mail2.vcu.edu. Phone: (804) 828-9482. Fax: (804) 828-3093.

‡ Cornell University.

§ Institute for Structural Biology and Drug Discovery, Virginia Commonwealth University.

|| Department of Biochemistry, Virginia Commonwealth University.

[1] Abbreviations: SHMT, serine hydroxymethyltransferase; rcSHMT, rabbit cytosolic SHMT; scSHMT, sheep cytosolic SHMT; hcSHMT, human cytosolic SHMT; mcSHMT, mouse cytosolic SHMT; eSHMT, *E. coli* SHMT; bsSHMT, *B. stearothermophilus* SHMT; PLP, pyridoxal 5′-phosphate; H_4PteGlu, tetrahydrofolate; CH_2-H_4PteGlu, 5,10-methylene-H_4PteGlu; CH^+-H_4PteGlu, 5,10-methenyl-H_4PteGlu; 5-CHO-H_4-PteGlu, 5-formyl-H_4PteGlu; CHOH-H_4PteGlu, N5-hydroxymethylene-H_4PteGlu; SHMT·Quin, intermediate between enzyme and glycine absorbing near 500 nm.

10.1021/bi049791y CCC: $27.50
Published on Web 05/11/2004

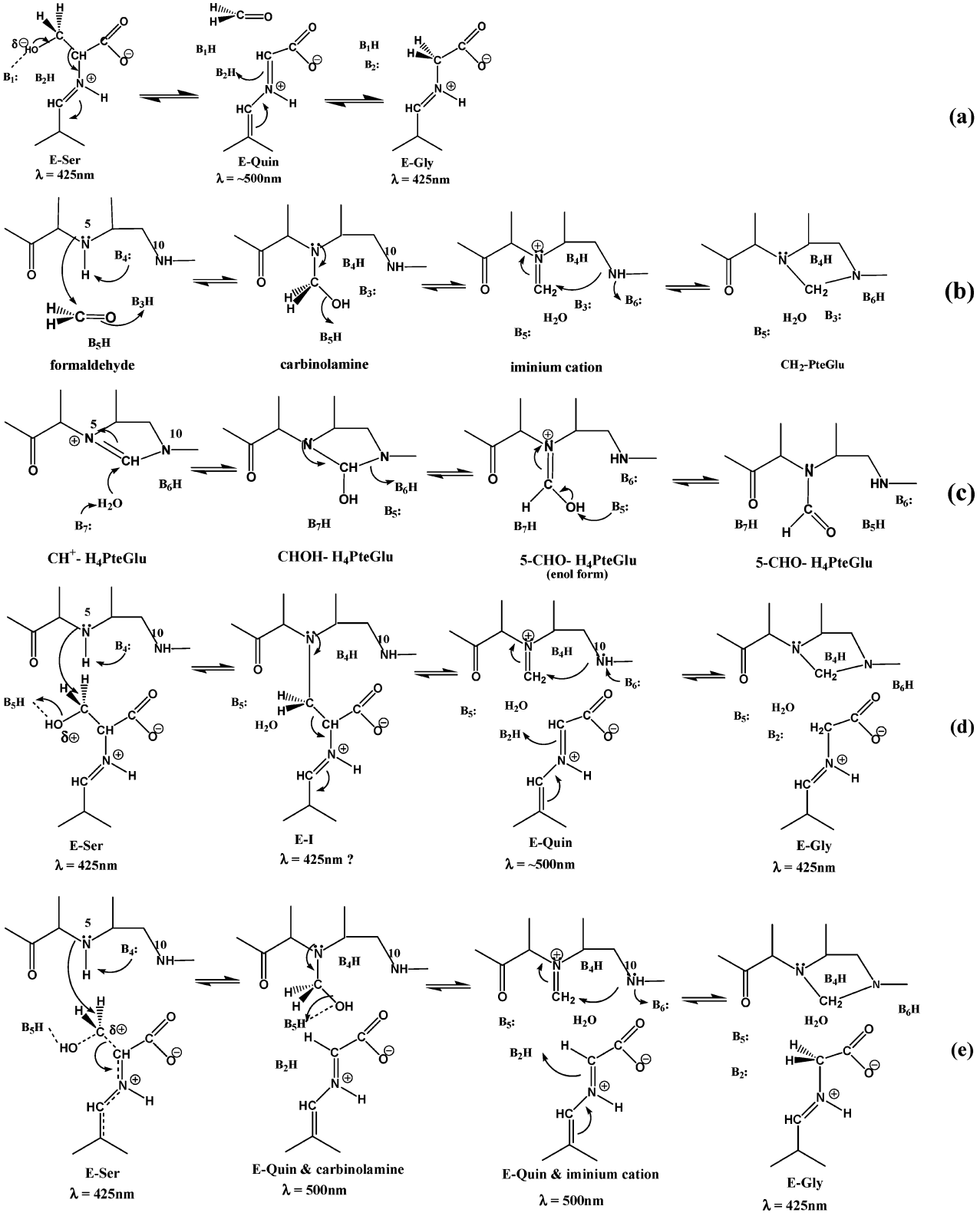

FIGURE 1: Proposed mechanisms for reactions catalyzed by SHMT and the requirement for general acid−base catalytic groups, labeled B_1−B_7. (a) Retroaldol mechanism for conversion of the serine internal aldimine to the glycine aldimine with formation of formaldehyde. E-Quin is the quinonoid intermediate and absorbs near 500 nm with a molar absorption coefficient of ~40000 cm^{-1} M^{-1}. B_1 is the putative base required to accept the proton from the C3 hydroxyl group. (b) Condensation of formaldehyde (generated as shown in panel a) with H_4PteGlu to form CH_2-H_4PteGlu. Only a portion of the H_4PteGlu structure is shown. The carbinolamine and iminium cation are intermediates in the formation of CH_2-H_4PteGlu. (c) Proposed mechanism for conversion of CH^+-H_4PteGlu to 5-CHO-H_4PteGlu with the formation of the intermediate CHOH-H_4PteGlu. This reaction requires glycine as a ligand even though the glycine is not consumed. (d) Nucleophilic displacement mechanism for the serine to glycine reaction. As in panel a, the first structure is the external aldimine of serine. It is not known at what wavelength the putative covalent adduct labeled E-I would absorb, but from its structure it is most likely around 425 nm. The intermediate labeled E-Quin is the same structure shown in panel a. (e) A concerted mechanism that combines the reactions shown in panels a and b. Formaldehyde may be formed transiently in this mechanism if breaking of the bond between C2 and C3 of serine precedes formation of a bond between N5 of H_4PteGlu and C3 of serine.

instead of formaldehyde. Subsequent studies have provided evidence that the formation of 5-CHO-H_4PteGlu$_n$ plays an important regulatory role in 1-C metabolism (*5*−*7*).

Three-dimensional structures have been determined for the cytosolic isozymes of human, rabbit, and mouse SHMT, as well as for SHMT from the prokaryotes *Escherichia coli* and *Bacillus stearothermophilus* (*8*−*12*). The active sites from these structural studies show conservation of key residues. Many of these residues have been changed by site-directed mutagenesis, and their role in binding and catalysis has been discussed. It has been suggested that the residues involved in the condensation of formaldehyde with H_4PteGlu$_n$ to form CH_2-H_4PteGlu$_n$ (Figure 1b; the second step in folate-dependent conversion of serine to glycine) are the same as in the hydrolysis of CH^+-H_4PteGlu$_n$ to 5-CHO-H_4PteGlu$_n$ (Figure 1c) (*13*, *14*). However, structural studies have been inconclusive regarding the role of various residues in reactions catalyzed by SHMT, and have not established whether formaldehyde is involved as an intermediate. Stereochemical considerations have raised doubts that formaldehyde is an intermediate, and the structure of a complex of serine with *B. stearothermophilus* SHMT supported a proposed mechanism in which N5 of H_4PteGlu$_n$ makes a nucleophilic displacement of the serine hydroxyl to form a covalent adduct between H_4PteGlu$_n$ and serine (Figure 1d) (*12*, *15*). This intermediate collapses into products without the involvement of formaldehyde as an intermediate. Key differences between the retroaldol mechanism and this nucleophilic displacement mechanism include the geometry of reactive groups around the serine, the presence or absence of free formaldehyde, and the role of acid−base groups.

The purpose of this study is to elucidate the role of Glu75 in rcSHMT by site-directed mutagenesis and structure determination. Glu75 could act as a proton donor or acceptor; it is situated at the active site, within hydrogen bonding distance of the C3 serine hydroxyl in a serine−SHMT complex and of the formyl oxygen of 5-CHO-H_4PteGlu in a complex of this species with SHMT. Spectral and kinetic work on several mutants of Glu75 in scSHMT has determined that this residue plays an important role in the mechanism of the folate-dependent serine-to-glycine reaction (*16*), and structural studies on eSHMT suggest that Glu75 (Glu57 in eSHMT) is protonated (*11*). The work presented here confirms the importance of Glu75 in the folate-dependent cleavage of serine (as a general acid−base catalyst) and establishes that it is not required for folate-independent allothreonine cleavage. In addition, it is clear that Glu75 is essential for the conversion of CH^+-H_4PteGlu$_n$ to 5-CHO-H_4PteGlu$_n$. The results are discussed in view of possible mechanisms for these reactions.

EXPERIMENTAL PROCEDURES

Materials. All amino acids, coenzymes, antibiotics, and buffers were obtained from Sigma (St. Louis, MO) or Fisher Scientific (Pittsburgh, PA). (6*S*)-H_4PteGlu and (6*S*)-5-CHO-H_4PteGlu were gifts from Eprova AG (Schaffhausen, Switzerland). Crystallization buffers were from Hampton Research (Laguna Niguel, CA).

Site-Directed Mutagenesis. Mutants of rcSHMT were made using the QuickChange site-directed mutagenesis kit from Stratagene (La Jolla, CA) on rcSHMT cDNA in the pET22b vector as described previously (*17*). Each mutation was confirmed by sequencing the cDNA insert in both directions. Each mutant protein was expressed in an *E. coli glyA*$^-$ strain as previously described (*17*). Purification was done by the same procedure published previously and resulted in high yields of >95% pure enzymes that exhibited the size and spectral characteristics of wild-type rcSHMT.

Kinetic Studies. All spectra and steady state kinetic studies were performed in a cell with a path length of 1 cm with an Agilent 8354 spectrophotometer at 30 °C. The buffer was either 20 mM potassium phosphate or sodium *N*,*N*-bis(2-hydroxyethyl)-2-aminoethane sulfonate (pH 7.3) unless otherwise noted. Catalytic activities for the cleavage of serine in the presence of H_4PteGlu and allothreonine in the absence of H_4PteGlu were performed as previously described (*18*).

Dissociation constants[2] for serine, glycine, and 5-CHO-H_4PteGlu were determined from double-reciprocal plots of the change in absorbance at 498 nm versus the change in the ligand concentration (*19*). The ligand concentrations were varied over a 10-fold range that bracketed the respective K_d values. For determination of the K_d for 5-CHO-H_4PteGlu, the glycine concentration was held constant at 100 mM.

The enzymatic rate of conversion of 5,10-CH^+-H_4PteGlu to 5-CHO-H_4PteGlu was determined by adding 50 mM glycine to the reaction mixture and observing the increase in absorbance at 502 nm, where the SHMT·Gly·5-CHO-H_4-PteGlu ternary complex absorbs with a molar absorption coefficient of 40 000 M^{-1} cm^{-1} (*2*, *3*). These reactions were performed at 20 °C because the increase in A_{502} was much greater upon formation of the ternary complex than at higher temperatures.

The rate of conversion of L-serine to enzyme-bound glycine and formaldehyde was determined on an Applied Photophysics SX.18MV stopped-flow spectrophotometer. SHMT (9.0 mg/mL) was flowed against 200 mM L-serine at 30 °C, and the rate of formation of the SHMT·Quin complex absorbing at 498 nm was observed. The kinetic traces were fit using software provided by Applied Photophysics. The rate of formaldehyde release was followed by trapping the formaldehyde with Schiff's reagent and determining the absorbance at 550 nm as previously described (*20*). A standard curve of formaldehyde and excess Schiff's reagent was used to convert absorbance into nanomoles of formaldehyde.

Crystallization. Crystallization was performed at room temperature by the hanging drop vapor diffusion technique. Crystals of both mutants were obtained by mixing 3 μL of an enzyme solution [34−44 mg/mL in 20 mM potassium phosphate (pH 7.3) with 1 mM dithiothreitol] with an equal volume of reservoir solution. The reservoir solution for E75L rcSHMT consisted of 50 mM potassium phosphate (pH 6.6), 8.5−9.1% PEG 8000, and 100 mM KCl. For E75Q rcSHMT, the reservoir solution consisted of 15 mM potassium 2-(*N*-morpholino)ethanesulfonate (pH 6.4), 8.5−10% PEG 4000, and 30 mM KCl. Serine complexes were formed by adding 0.25 μL of 250 mM L-serine directly to the drop, giving an ~10 mM L-serine solution. Each mutant enzyme and the serine complexes formed yellow tetragonal bipyramidal crystals that reached a maximum size of ~0.7 mm × ~0.4

[2] These are apparent K_d values as at least two steps are involved in forming the E·Quin complex.

mm × 0.2 mm in 2−3 days. To obtain a ternary complex, crystals formed from the enzyme and serine were soaked for a few minutes in a solution containing 1 mM (6*S*)-H_4-PteGlu. Prior to data collection, crystals were washed with a solution of 8% PEG 4000, 100 mM KCl, and 50 mM potassium phosphate (pH 6.6). The wash was followed by a quick transfer to a series of solutions containing 15, 23, and 27% PEG 4000 and finally 27% PEG 4000 and 23% glycerol. The crystals were then rapidly frozen in liquid N_2.

Determination of the Structure. Data were collected from crystals of the E75Q and E75L mutants, with and without serine present; a partial data set was also obtained for E75L rcSHMT crystals soaked in serine and H_4PteGlu (E75L-Ser-H_4PteGlu set). All crystals were isomorphous with each other and with wild-type crystals; differences in unit cell dimensions were slight. The space group was $P4_12_12$. Images were integrated with mosflm (*21*) and scaled with scala (*22*), using the DPS (*23*) interface. Initial structures were determined by rigid body refinement of either the wild-type structure or a previously refined mutant structure; the crystallographic *R* at this stage was between 0.23 and 0.30, depending on the degree of similarity between the starting model and the structure being determined. Manual adjustments in the region of the mutation were made, and refinement was carried out using CNS (*24*) (for grouped *B*-factor refinement and atomic position refinement using energy minimization) and O (*25*) (for manual adjustments, and addition of water molecules).

Multiple cycles of refinement, and placement of water molecules, were carried out for the two higher-resolution data sets (E75L-Ser and E75Q). These structures were then used as starting points for the corresponding lower-resolution structures (E75L and E75L-Ser-H_4PteGlu, and E75Q-Ser, respectively). In the case of E75L-Ser-H_4PteGlu, the data were insufficient for complete refinement; a single cycle was carried out, followed by calculation of a difference map. Accurate determination of this structure will require further data collection. For E75L and E75Q-Ser, refinement was successfully carried out, although no attempt was made to modify the solvent structure in these lower-resolution cases. Final difference electron density maps for the four refined structures did not contain any significant features.

The mammalian SHMT structure is a homotetramer, which may be described as a dimer of dimers. In the structures presented here, the asymmetric unit contains one tight dimer, made up of chains A and B; the second dimer is related to the first by a crystallographic symmetry operation. We use a residue numbering scheme based on the human SHMT sequence to facilitate comparison with other mammalian enzymes. With this scheme, each final structure includes residues 15−275 and 283−484 in chain A and residues 15−277 and 282−484 in chain B. Missing residues, at the N-terminus and in the middle of a flexible loop, do not appear to play any role in molecular function. The dimer also includes two PLP molecules, each of which is primarily associated with one chain but also contacts residues from the second chain. The amino acid binding site involving the PLP primarily associated with chain A is designated site I, and the second site is site II. Approximately 100 water molecules are included, and one phosphate ion is present in most of the amino acid binding sites.

E75Q has three water molecules in one of its amino acid binding sites and a phosphate ion in the other. For E75Q-Ser, an omit map calculated with omission of these solvent molecules clearly indicated the presence of glycine (or possibly disordered serine) in one of the two sites, and subsequent refinement included a Gly in this position. The amino acid binding sites of E75L-Ser contain primarily PO_4^{2-}, and the E75L model included these ions from the beginning.

The original determination of the wild-type rcSHMT structure (*9*) was in space group $P4_12_12$, with one tight dimer per asymmetric unit. In a subsequent, higher-resolution, structure of an rcSHMT−H_4PteGlu complex, the lower $P4_1$ symmetry was found, with a pair of dimers in the asymmetric unit (*26*). To verify the space group for these crystals, the data were reprocessed in space group $P4_1$. There was no significant improvement in *R*-factors, and the conformation of the two dimers remained the same. We conclude that, to the resolution of the current data, $P4_12_12$ symmetry is preserved for the E75L and E75Q mutants. Statistics from data collection and processing, and structure determination, are summarized in Table 1. Coordinates have been deposited in the Protein Data Bank (*27*), as entries 1RV3 (E75L-Ser), 1RV4 (E75L), 1RVU (E75Q), and 1RVY (E75Q-Ser).

RESULTS

Spectral Properties of rcSHMT Mutants E75Q and E75L. The mutant enzymes were expressed and purified by the same procedure used for recombinant wild-type rcSHMT. The enzymes are yellow, exhibiting a single absorption maximum above 300 nm at 428 nm with a 278 nm:428 nm ratio of 6.2. The mutant enzymes were stable at −20 °C for several months. Glycine, added to saturating conditions, resulted in three observable absorption maxima at 498, 425, and 343 nm. These absorption maxima reflect three intermediates on the reaction pathway. The 343 nm peak is the *gem*-diamine, which occurs as the first covalent complex of the enzyme (*28*). This is followed by formation of the external aldimine complex, absorbing at 425 nm, which is shown as the first and last structures in Figure 1a for serine and glycine, respectively. The 498 nm-absorbing species is the quinonoid complex, in which a pair of electrons on C2 of glycine are in resonance with the π-electron system of the bound pyridoxal phosphate (*28*). This structure is labeled E·Quin in Figure 1a. The spectra of both the E75Q and E75L glycine complexes are very similar to the spectrum of the wild-type rcSHMT·Gly complex. The major difference between the mutant and wild-type enzymes is that the absorption peak near 500 nm is severalfold higher. As with the wild-type rcSHMT·Gly complex, lower temperatures and higher pH values shift the equilibrium from the aldimine complex to the *gem*-diamine complex. By titrating the enzyme with glycine and determining the increase in absorption at 498 nm, we were able to determine a K_d value for glycine for each mutant rcSHMT (Table 2). The affinity for glycine was nearly normal for E75Q, but was almost 8-fold lower for E75L.

The addition of either H_4PteGlu or 5-CHO-H_4PteGlu to the mutant rcSHMT·Gly complexes resulted in a severalfold increase in the absorption of the 500 nm peak at 20 °C. This is also observed with wild-type rcSHMT. This spectral effect of 5-CHO-H_4PteGlu permitted a determination of the K_d value for 5-CHO-H_4PteGlu for both E75Q and E75L

Table 1: Summary of Data Collection, Data Reduction, and Structure Refinement[a]

	E75L	E75L-Ser	E75L-Ser−H_4PteGlu	E75Q	E75Q-Ser
	Data Collection and Initial Processing				
unit cell dimensions *a*, *c* (Å)	115.0, 158.4	114.9, 158.3	114.7, 158.0	114.6, 156.8	114.7, 156.4
resolution (Å)	36−2.95	49−2.40	49−2.95	58−2.50	27−2.90
R_{sym}	0.116 (0.553)	0.100 (0.566)	0.166 (0.669)	0.111 (0.544)	0.188 (0.626)
$I/\sigma(I)$	6.1 (1.4)	6.0 (1.3)	3.4 (1.0)	6.4 (1.4)	3.8 (1.1)
completeness (%)	99.9	99.8	73.4	99.6	93.8
redundancy	9.0	13.0	5.3	5.3	5.8
no. of observations	207374	547673	87974	195522	130399
no. of unique reflections	23067	42006	16463	36699	22342
	Structure Determination and Refinement				
R/R_{free}	0.201/0.245	0.224/0.255	0.226/0.310	0.221/0.253	0.220/0.283
average *B*	50	49	66	37	34
total no. of reflections	22868	41555	16382	36655	22026
no. of reflections in the test set	1113	2087	795	1843	1242
total no. of non-H atoms	7310	7310	7344	7326	7328
no. of water molecules	86	86	86	105	102
rmsd from ideal geometry					
bond lengths (Å)	0.007	0.007	0.008	0.007	0.007
bond angles (deg)	1.35	1.34	1.33	1.32	1.34

[a] Data were collected at the Cornell High Energy Synchrotron Source (CHESS), station A-1, for E75L, E75L-Ser, and E75L-Ser−H_4PteGlu crystals, and on a rotating anode generator for E75Q and E75Q-Ser crystals. A single crystal was used for each collection, except for E75L-Ser−H_4PteGlu, for which two crystals were used. The detector was an ADSC Quantum-210 instrument at CHESS and a Rigaku R-axis instrument in the home lab. Values of R_{sym} and $I/\sigma(I)$ are given as the overall values (values for the highest-resolution shell in parentheses).

Table 2: Kinetic Constants for rcSHMT Mutant Enzymes (30 °C)

constant	wild-type rcSHMT	E75L	E75Q
K_m (Ser) (mM)	0.8	27[a]	4.0
K_d (Gly) (mM)	6	45	7.7
K_d (5-CHO-H_4PteGlu) (μM)	10	26	10
k_{cat} (Ser) (min^{-1})	600	not detectable	1.2
K_m (alloThr) (mM)	1.5	22	15
k_{cat} (alloThr) (min^{-1})	130	144 (110%)[b]	560 (430%)[b]
$k_{E\cdot Quin}$ (min^{-1})	not determined	64 and 23[c]	460 and 11
k_{HCHO} (min^{-1})	0.0028[d]	0.34[d]	0.13

[a] This is a K_d value. [b] Percentage of the wild-type value in parentheses. [c] Biphasic rate constants for formation of E·Quin from serine absorbing at 498 nm. [d] Estimate of the rate of formation of HCHO from serine as determined from the initial rate.

rcSHMT (Table 2). Compared to wild-type rcSHMT, E75L rcSHMT has a 2.5-fold lower affinity for 5-CHO-H_4PteGlu while E75Q rcSHMT has the same affinity.

Saturation of wild-type rcSHMT with L-serine also results in the three absorption maxima at 343, 425, and 498 nm, but the intensity of the 343 and 498 nm peaks is greatly diminished compared to those observed with glycine (*28*). However, with both E75Q and E75L rcSHMT, saturation with serine results in significant absorption maxima at 343 and 498 nm (the absorption maximum with E75L rcSHMT is actually at 502 nm) (Figure 2). Again, at lower temperatures or higher pH, the equilibrium is shifted toward the *gem*-diamine intermediate absorbing at 343 nm. Titration of E75Q and E75L rcSHMT with serine permitted determination of their respective K_d values via a plot of the reciprocal increase in A_{498} against the reciprocal serine concentration (Table 2). E75Q and E75L rcSHMTs had 5- and 30-fold reduced affinity for serine, respectively, compared to the wild-type enzyme.

Kinetic Constants for E75Q and E75L rcSHMT with Serine and Allothreonine. Attempts were made to determine K_m and k_{cat} values for the conversion of serine and H_4PteGlu to glycine and 5,10-CH_2-H_4PteGlu by the normal assay procedure. With E75L rcSHMT, there was no detectable activity, but with a high concentration of E75Q, activity was observed and a k_{cat} value of 1.2 min^{-1} was determined, assuming that both serine and H_4PteGlu were at saturating concentrations (serine at 50 mM and H_4PteGlu at 0.2 mM) (Table 2). This represents a 500-fold decrease in activity compared to that of the wild-type enzyme. In contrast, both mutant enzymes exhibited greater catalytic activity with allothreonine in the absence of H_4PteGlu than the wild-type enzyme (Table 2). The K_m values for allothreonine are increased by a factor of

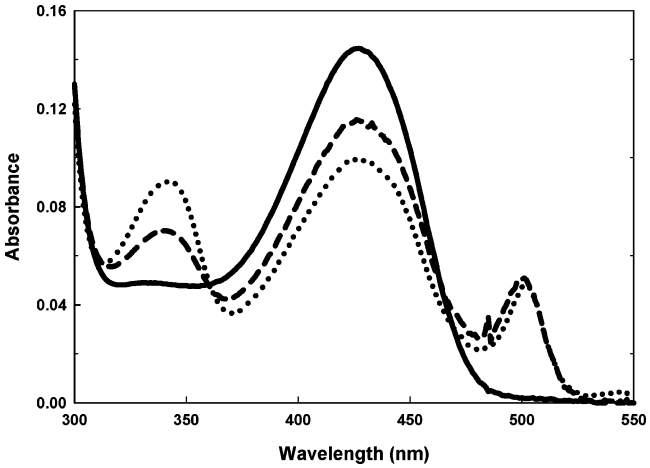

FIGURE 2: Spectra of E75L rcSHMT as a function of serine concentration and temperature: (—) 1.2 mg/mL E75L rcSHMT at pH 7.6, (···) after the addition of L-serine to a final concentration of 60 mM at 7 °C, and (- - -) same solution but at 37 °C.

~10, while the k_{cat} value for E75Q rcSHMT is more than 4-fold higher than that of the wild-type enzyme. If allothreonine is processed by the retroaldol cleavage mechanism shown in Figure 1a, and serine (in the presence of H_4PteGlu) is processed by the same mechanism followed by the condensation of formaldehyde with H_4PteGlu (Figure 1b), then these results strongly suggest that Glu75 is associated with the condensation step and not with the retroaldol cleavage step. If the mechanisms are not the same, Glu75 is clearly implicated in the one which operates in the presence of folate.

We had previously investigated the ability of rcSHMT to cleave serine to glycine and formaldehyde in the absence of H_4PteGlu (*29*). We showed that this did occur very slowly, with a k_{cat} of 0.0028 min^{-1}. Evidence suggested that the rate-determining step was the release of formaldehyde and not serine cleavage (*30*). Both E75Q and E75L rcSHMT saturated with serine show a significant absorption peak near 500 nm that is not seen with wild-type rcSHMT at pH <7.0, but can be detected in the wild-type enzyme as a small peak at higher pH values (*31*). This absorption peak represents the quinonoid structure and is shown as E·Quin in Figure 1a. This intermediate can exist only if serine has been cleaved to glycine and formaldehyde. The rate of formation of E·Quin for E75Q and E75L rcSHMT was determined by observing the increase in absorbance at 498 nm in the presence of a saturating concentration of L-serine, by stopped-flow spectrophotometry. For each mutant enzyme, the rate was fit by a double-exponential equation. For E75Q rcSHMT, the rates were 460 and 11 min^{-1} with relative amplitudes of 61 and 39%, respectively (Table 2). For E75L rcSHMT, the biphasic curve gave values for *k* of 64 and 23 min^{-1} with relative amplitudes of 42 and 58%, respectively. Because the amplitude of the 498 nm absorption peak with wild-type rcSHMT is so small, the rate of its formation could not be determined by this method.

The appearance of the absorption peak near 500 nm raises the question of how fast formaldehyde is being formed by E75Q and E75L rcSHMT. As noted above, with wild-type rcSHMT, the value is 0.0028 min^{-1}. Since both E75L·Ser and E75Q·Ser complexes exhibit a greater concentration of the quinonoid intermediate than wild-type SHMT, it seemed likely that the rate of formation of glycine and formaldehyde would be significantly increased. We determined the rate of formation of formaldehyde by taking aliquots every few minutes of a solution containing enzyme and saturating serine and using Schiff's reagent to determine the formaldehyde concentration. We found that formaldehyde was formed but that the rate rapidly decreases with time, suggesting that the released formaldehyde inactivates the enzyme (Figure 3a). Using the first data point, at 3 min, we calculated $k_{cat,app}$ values for E75Q and E75L rcSHMT of 0.13 and 0.34 min^{-1}, respectively (Table 2). These are minimum rate constants, since we are unable to obtain a true initial rate. These rates are much slower than the rate of appearance of E·Quin, which suggests that formaldehyde release is rate-limiting for the overall reaction, as found for wild-type rcSHMT (*30*).

SHMT-Catalyzed Formation of 5-CHO-H_4PteGlu. In addition to catalyzing the interconversion of serine and glycine, SHMT catalyzes the formation of 5-CHO-H_4PteGlu, and its polyglutamate forms, from 5,10-CH^+-H_4PteGlu (Figure 1c). Arguments have been made that the acid−base chemistry

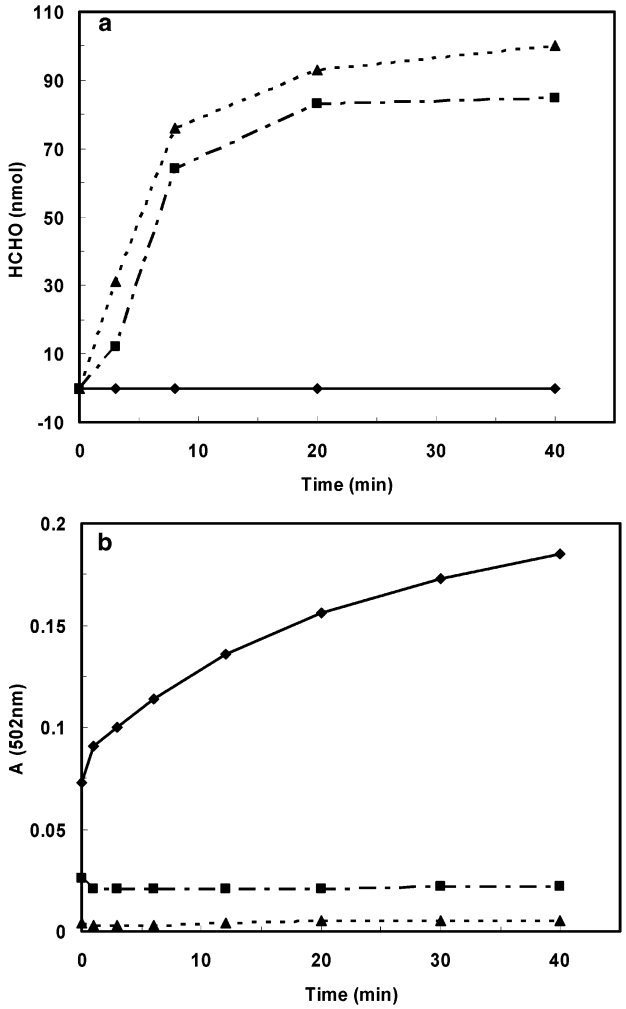

FIGURE 3: Catalytic activity of rcSHMT and Glu75 mutants in the folate-independent conversion of serine to glycine and formaldehyde and the hydrolysis of CH^+-H_4PteGlu to 5-CHO-H_4PteGlu. (a) Formaldehyde formation with only serine as the substrate: (▲) formaldehyde formation with 30 nmol of E75L SHMT, (■) formaldehyde formation with 30 nmol of E75Q SHMT, and (◆) formaldehyde formation with wild-type rcSHMT. (b) Appearance of the SHMT·Gly·5-CHO-H_4PteGlu ternary complex absorbing at 502 nm with (▲) E75L SHMT, (■) E75Q SHMT, and (◆) wild-type rcSHMT.

involved in this reaction, in which the 1-C group is at the oxidation level of formate instead of formaldehyde, mimics the acid−base catalysis of the formation of 5,10-CH_2-H_4-PteGlu from formaldehyde and H_4PteGlu (*13*, *14*). To test this, we determined the ability of E75Q and E75L rcSHMT to catalyze the reaction shown in Figure 1c, including the intermediate hydroxymethylene derivative shown as CHOH-H_4PteGlu. The maximum amount of this intermediate forms when CH^+-H_4PteGlu is incubated at pH 4.0 (*14*). The rate-determining step for the enzymatic formation of 5-CHO-H_4-PteGlu is the formation of this intermediate, which is rapidly converted to product by rcSHMT. The reaction requires glycine, and product formation is monitored by the appearance of the 502 nm-absorbing rcSHMT·Quin·5-CHO-H_4-PteGlu complex (Figure 1a).

Figure 3b shows the increase in absorbance at 502 nm when an aliquot of a concentrated solution of CH^+-H_4PteGlu at pH 4.0 is added to 0.8 mL of the rcSHMT·Gly complex and the mutant proteins E75Q and E75L rcSHMT at pH 7.2 and 20 °C. With wild-type rcSHMT, there is a rapid burst

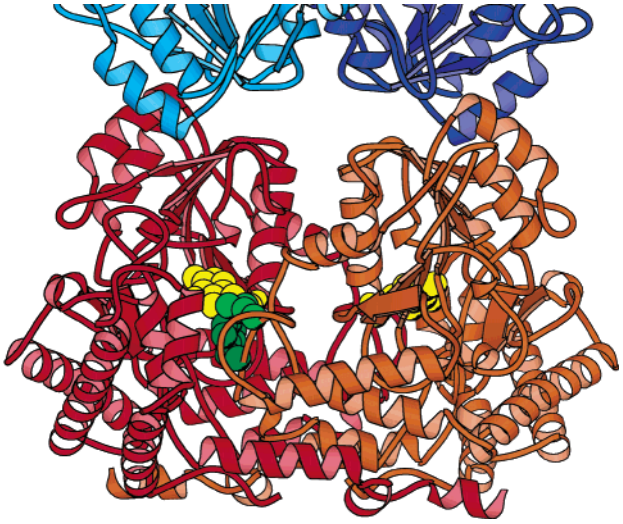

FIGURE 4: Overall view of the E75L-Ser•SHMT structure. Chain A (red) and chain B (orange) make up a tight dimer. A symmetry-related dimer, which makes up the other half of the biologically active tetramer, is partially visible, in shades of blue, at the top of the figure. PLP molecules are shown in yellow space-filling form. Leu75′ and its neighbor Tyr73′ are also shown in space-filling form for site I, in light and dark green, respectively. The figure was drawn with Molscript (*32*).

in the rate of formation of 5-CHO-H_4PteGlu, as indicated by the appearance of absorbance at 502 nm (Figure 3b). This has been shown to result from the conversion of the intermediate CHOH-H_4PteGlu, which exists in equilibrium with CH^+-H_4PteGlu at this pH, to 5-CHO-H_4PteGlu. When wild-type rcSHMT was replaced with E75Q and E75L rcSHMT in this assay, there was only a very small, rapid increase in absorbance at 502 nm, most notable with E75L rcSHMT (Figure 3b). At this temperature and pH, the absorbance of the ternary complex with glycine and 5-CHO-H_4PteGlu is similar in intensity to that observed with the wild-type enzyme. We conclude that the Glu75 mutants do not catalyze the formation of 5-CHO-H_4PteGlu from either CH^+-H_4PteGlu or CHOH-H_4PteGlu. The small increase in absorbance at 502 nm seen with the mutant rcSHMTs may be the result of a small amount of 5-CHO-H_4PteGlu in our stock CH^+-H_4PteGlu solution at pH 4.0.

Structure of E75Q and E75L rcSHMT. The overall structure of both mutants is very similar to that of the wild-type protein, in keeping with earlier observations that SHMTs from different species, and with different substrates bound, exhibit only small differences in conformation (*7*−*12*, *26*). The overall structure is shown in Figure 4, and localized differences around the mutation site in Figure 5. In Figure 5, and in the following discussion of active site residues, those with a prime belong to chain B for site I and chain A for site II. Besides the actual mutated side chain of residue 75′, the most obvious differences are in nearby tyrosine residues 73′ and 83′.

In E75Q, the side chain of Gln75′, unlike the extended side chain of wild-type Glu75′, is bent back toward the main chain, and a hydrogen bond is made between OE1 and the amide N of the same residue. Two water molecules (which are not present in E75L) help to stabilize this conformation. Differences between wild-type and E75Q Tyr73′ and Tyr83′ are visible, but small, and the hydrogen bonding network in the vicinity of the active site is maintained, except for residue 75′ itself.

In E75L, Leu75′ is displaced (∼1 Å at C_α) relative to its position in E75Q. This shift is accomplished by small rotations of main chain torsion angles from approximately residue 70′ to 76′, particularly noticeable at the peptide bond between residues 74′ and 75′, and serves to reduce the exposure of the hydrophobic side chain to solvent. Tyr73′ is affected by this shift; its C_α is also displaced ∼1 Å. To compensate, the tyrosine side chain is rotated toward Leu75′, placing its aromatic ring in approximately the same place as in E75Q. However, its orientation is different, and its OH can no longer make an H-bond to OP2 of PLP. In this position, the tyrosine OH is close to the amino acid binding site and would be expected to affect the binding and reaction of serine and other amino acids. A smaller motion of the Tyr83′ side chain, which is adjacent to that of Tyr73′, is also observed.

In both amino acid binding sites of E75L, and in one site of E75Q, there appears to be a large solvent species, probably a phosphate ion. Previous studies have shown that anions, such as phosphate, are competitive inhibitors of binding of serine and glycine to rcSHMT (*34*). Hydrogen bonds are formed between this PO_4^{2-} and surrounding residues Ser53, Arg402, and Tyr83′; in E75L, there is also an H-bond to Tyr73′ (which may help to account for the conformation of this residue). Site I in E75Q is occupied by a trio of water molecules, one of which makes H-bonds to Ser53 and Tyr83′.

E75L-Ser does not actually contain a well-defined serine in the crystal structure. In fact, both binding sites seem to be primarily occupied by phosphate. An omit map (leaving out the PO_4^{2-} ions) does show a connection between the feature at the PO_4^{2-} location in site II and C4A of the adjacent PLP, indicating possible partial occupancy by serine or glycine. Because of the superimposed phosphate, it is not possible to make an accurate model of this species. Close examination of the residues surrounding site II indicates that the side chain of Tyr73′ is poorly ordered; it probably has a different conformation when an amino acid is bound. The quality of the E75L-Ser−H_4PteGlu map is inadequate for determining what species are bound in the amino acid binding sites. There is some density in the expected location for a bound folate in one of the two possible sites (site I), which is consistent with the previous finding that 5-CHO-H_4PteGlu$_3$ binds in only one site per dimer (*26*).

E75Q-Ser also does not appear to contain well-ordered serine. However, an omit map of the site I region contains density consistent with a bound glycine; site II appears to be occupied by PO_4^{2-}. Although the Gly carboxyl is quite clear in the map, density for C_α is weak, indicating that multiple conformations may be present. Accordingly, both *gem*-diamine and external aldimine forms of glycine were built, with the carboxyl groups of the two species in approximately the same location but the C_α atoms well separated (Figure 6). The limited resolution of the data does not permit great accuracy in determining the Gly conformation, but it does appear that the preferred position of the carboxyl group is not consistent with the formation of a pair of H-bonds to Arg402 [as seen in eSHMT (*11*), bsSHMT (*12*), and sites I and II of mcSHMT (*10*)]. Instead, H-bonds are formed to Tyr83′, Gln75′, and Arg402 (*gem*-diamine, only one H-bond) or Ser53 (aldimine). These patterns are

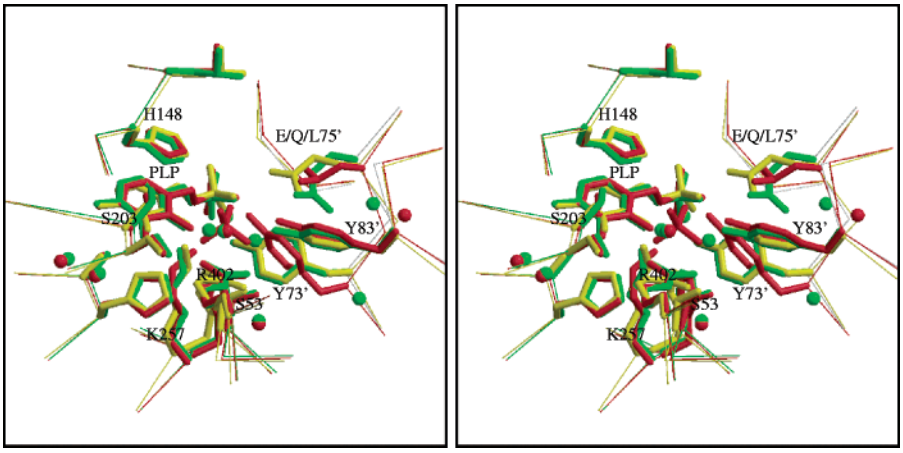

FIGURE 5: Stereoview comparing wild-type, E75L, and E75Q amino acid binding site I. The main chain within approximately 8 Å of the site is shown as a thin C_α trace, and side chains are shown in stick form. Water molecules appear as isolated spheres. The wild-type structure is in yellow, E75Q in green, and E75L in red. Site II is very similar, except that E75Q has a central phosphate ion instead of water. In this view, an entering folate would come in from the top. This figure was drawn using Molscript (*32*) and Raster3D (*33*).

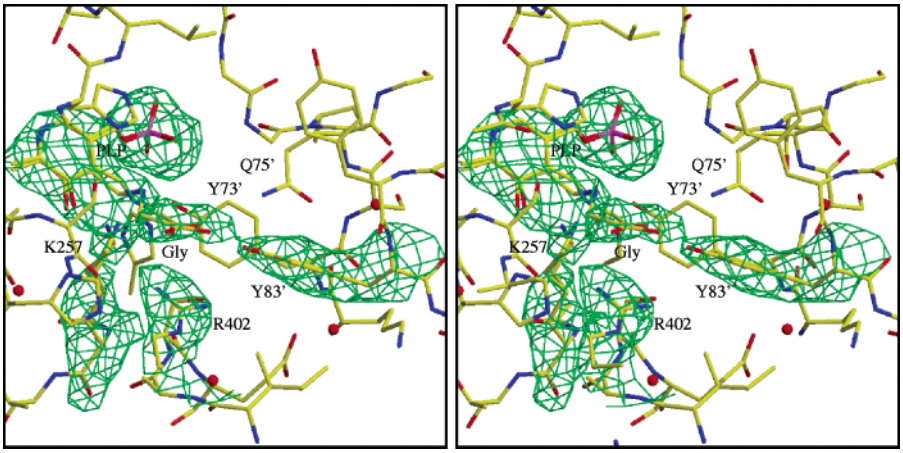

FIGURE 6: Stereoview of bound glycine in E75Q-Ser site I. *gem*-Diamine and external aldimine forms, and the corresponding Lys257 side chain conformations, are overlaid. The color code for atom types is as follows: yellow for C, blue for N, red for O, and magenta for P. A difference electron density map produced by omitting PLP-Gly and a shell of neighboring protein residues is in green. The contour level is 2.8σ, and only density surrounding PLP-Gly and the nearby Tyr83′ and Arg402 residues is drawn. This figure was drawn using Molscript (*32*) and Raster3D (*33*).

similar to those observed in mcSHMT sites III and IV (*10*). The structure suggests that the conformation of PLP and the side chain of Lys257 may differ between E75Q and E75Q-Ser, and between *gem*-diamine and external aldimine forms of bound Gly, but higher-resolution data will be needed to confirm this. Aside from Lys257, protein residues surrounding site I exhibit no significant conformational differences between E75Q and E75Q-Ser.

The E75Q-Ser structure confirms that E75Q rcSHMT is capable of converting serine to glycine in the absence of folate, and that (at least in the crystal) the two binding sites in a mammalian SHMT dimer are not strictly equivalent (*8*, *26*). It is not possible to tell whether site II does not bind serine in the first place or whether it binds serine, converts it to glycine and formaldehyde, and then releases the products. Likewise in the E75L-Ser structure, the absence of serine could be due to a lower affinity for serine than for phosphate or to conditions favoring conversion to glycine and release of products.

DISCUSSION

There are two current views about the mechanism of SHMT which address its broad substrate and reaction specificity. One is that all reactions of 3-hydroxy amino acids can be explained by a common retroaldol-type mechanism, with an aldehyde as an intermediate in both the folate-dependent serine-to-glycine conversion and the folate-independent threonine and β-phenylserine reactions (Figure 1a). Similarly, the condensation of H_4PteGlu with formaldehyde and the conversion of CH^+-H_4PteGlu to 5-CHO-H_4PteGlu share a common mechanism (Figure 1b,c). A second view is that allothreonine and β-phenylserine cleavage occur by a retroaldol mechanism, but serine and H_4PteGlu are converted to products using a mechanism whose first step is a nucleophilic displacement of the C3 hydroxyl group of serine by N5 of H_4PteGlu, to form a serine−H_4PteGlu covalent intermediate; no formaldehyde is involved (Figure 1d) (*12*, *15*). All these mechanisms rely on acid−base chemistry, with protons being shuttled to and from the proposed intermediates by acid−base groups on protein residues around the active site, and by water molecules.

One particularly good candidate for the involvement in acid−base chemistry at the active site is Glu75 in rcSHMT (corresponding to Glu53 in bsSHMT, Glu57 in eSHMT, Glu74 in scSHMT, and Glu75 in hcSHMT and mcSHMT).

In scSHMT, mutation of this residue to Gln or Lys lowered the catalytic activity for serine in the presence of H_4PteGlu by ~300-fold, but had little effect on the rate of cleavage of allothreonine (*16*). This study did not measure the effect on the conversion of CH^+-H_4PteGlu to 5-CHO-H_4PteGlu, and a structure for this enzyme is not currently available. However, the work clearly established that Glu75 is an important catalytic residue.

Role of Glu75 As Determined from Spectral and Kinetic Properties of Mutants. Mutation of Glu75 did not significantly affect the spectral properties of either the free enzyme or the enzyme−glycine complex. However, the mutations did have a dramatic effect on the spectral properties of the enzyme−serine complex. The absorbance at 498 nm (502 nm for the E75L mutant) shows that some of the serine has been cleaved to enzyme-bound glycine (SHMT·Quin) and formaldehyde (Figure 2). We had previously shown that rcSHMT does slowly catalyze the (folate-independent) conversion of serine to glycine and formaldehyde, but the turnover number of 0.0028 min^{-1} was governed by the rate of release of formaldehyde rather than the cleavage of serine (*29*, *30*). We could make no statement in this previous study about how fast serine was cleaved to glycine and formaldehyde. With the Glu75 mutants, we show that formaldehyde release is greatly accelerated compared to that in wild-type rcSHMT, but is still very slow with rates of 0.34 and 0.13 min^{-1} for E75L and E75Q, respectively (Table 2). From the appearance of E·Quin absorption at 498 nm, the rate of serine cleavage could be determined directly, without regard for formaldehyde release; it was found to be as high as 64 and 460 min^{-1} for E75L and E75Q rcSHMT, respectively. The rate of 460 min^{-1} for the E75Q mutant is similar to the rate of cleavage of allothreonine, and approaches the k_{cat} value of 600 min^{-1} for the wild-type enzyme in the presence of H_4PteGlu (Table 2). We conclude from these results, supported by the crystal structures of the mutants, that the environment of the amino acid binding site and the role of PLP have not been altered significantly by changing Glu75 to either Gln75 or Leu75, and that the mutant enzymes are clearly competent for catalyzing folate-independent cleavage of 3-hydroxy amino acids, including serine. Therefore, the greatly reduced rate of the cleavage of serine and H_4PteGlu to glycine and CH_2-H_4PteGlu in the E75L and E75Q mutants must be associated with a step involving folate. This is further supported by the complete loss of the ability of the mutant enzymes to convert CH^+-H_4PteGlu to 5-CHO-H_4PteGlu (Figure 3b) (*13*, *14*).

Mechanistic Implications. Figure 1 shows some possible mechanisms for the reactions catalyzed by SHMT, along with the acid−base groups that are required for the proton transfer steps. From its location in SHMT·Ser and SHMT·Gly·5-CHO-H_4PteGlu complexes, we propose that Glu75 serves as both B_5 and B_6 in panels b and c of Figure 1.

The lowest-energy pathway for a retroaldol reaction requires the C3 hydroxyl of the substrate to be antiperiplanar to the amino group of the aldimine and the C2−C3 bond of serine to be perpendicular to the plane of the PLP ring (*35*). In a reaction starting with (3*R*)-[3-^{3}H]serine bound in the antiperiplanar conformation, it is predicted that the product will be (11*S*)-[11-^{3}H]CH_2-H_4PteGlu, if formaldehyde does not rotate, or a racemic mixture of 11*S* and 11*R* if it does rotate freely, as expected (*15*). However, two different research groups have shown that the principal product is in fact labeled at the 11*R* position (*36*, *37*). Moreover, the 1.9 Å structure of the bsSHMT·Ser complex (the only structure reported to date for an SHMT·Ser complex) (*12*) shows clearly that the hydroxyl group of serine is synperiplanar. A retroaldol mechanism for serine in the synperiplanar conformation would give (11*R*)-[11-^{3}H]CH_2-H_4PteGlu, assuming that the intermediate formaldehyde does not rotate. The difficulty is then to explain (1) what keeps the formaldehyde from rotating and (2) how a rapid reaction rate can be achieved with this nonpreferred stereochemistry.

The first step of the retroaldol mechanism (Figure 1a) requires a base to abstract a proton from a 3-hydroxy group of an amino acid. Two studies looked at the effect of the substituent on the β-carbon (C3) of the amino acid on the rate of retroaldol cleavage in the absence of H_4PteGlu (*3*, *38*). Both studies came to the conclusion that electron-donating groups on C3 stabilize the transition state in the rate-determining step of the reaction. The resulting interpretation was that, for substituted 3-hydroxy amino acid substrates, such as allothreonine and β-phenylserine, the initial step in the mechanism could involve a transfer of the proton on O_γ to a base, forming either the alkoxide or a highly negative hydroxyl group (as shown in Figure 1a; B_1 is the base). However, crystal structures indicate that there is no suitable base near the 3-OH group of bound serine. Hydrogen bonding patterns from previous and current structural data suggest that Glu75 is probably in its acid form (*9*, *12*). It is likely to be the acid that donates a proton in the dehydration of CHOH-H_4PteGlu to form the iminium cation (B_5H in Figure 1b). Data from this study also indicate that Glu75 is required to catalyze the conversion of CH^+-H_4-PteGlu to 5-CHO-H_4PteGlu, as the E75Q and E75L mutants are nonfunctional for this reaction. This conversion requires the donation of a proton to N10 of the folate (Figure 1c), and structural analysis shows that Glu75 is in position to do this, further suggesting that it is in the conjugate acid form. Even if it is not protonated, it is not expected to be a strong base in the active site environment. Previous studies have also indicated that no other nearby basic group (the 5′-phosphate of PLP, His256, or His148) is a strong base (*39*−*42*).

All SHMTs that have been studied with respect to substrate specificity catalyze at significant rates the folate-independent retroaldol cleavage of both the *erythro* and *threo* isomers of the hydroxyl at C3, with the *erythro* isomer being favored. If *erythro*-β-phenylserine is modeled into the active site with the C3 hydroxyl synperiplanar, the phenyl ring occupies a cavity lined by residues His148, Leu149, Ser203, Glu75′, Tyr82′, Phe297′, and Gly302′. When the *threo* isomer is modeled with the same C3 hydroxyl conformation, there is considerable overlap of the phenyl group with residues Tyr73′ and Glu75′. Conversely, rotating the C3 hydroxyl to the antiperiplanar position allows the phenyl group of the *threo* isomer to fit into the cavity but creates steric clashes for the *erythro* isomer. The situation for threonine versus allothreonine is similar to that for *threo*- versus *erythro*-β-phenylserine. Hence, it appears that substrate cleavage can occur for both synperiplanar and antiperiplanar conformations. The lack of a strong base and the lack of stereospeci-

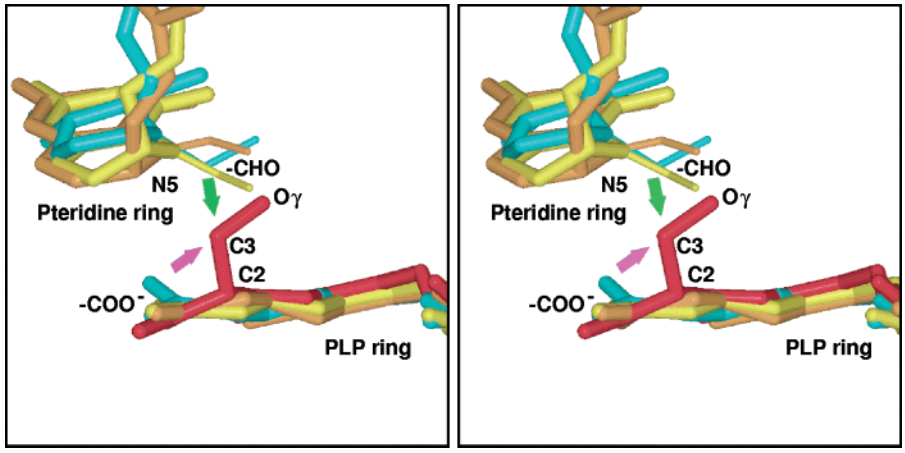

FIGURE 7: Stereoview of PLP, 5-CHO-H_4PteGlu, glycine, and serine at the active site in various SHMT structures. Orange, yellow, and cyan are for ternary complexes of SHMT with 5-CHO-H_4PteGlu and glycine (external aldimine form) from *B. stearothermophilus* (*12*), *E. coli* (*11*), and mouse (site I of cytosolic SHMT) (*10*), respectively. Red is for the binary complex of serine external aldimine with bsSHMT (*12*). The CHO group of 5-CHO-H_4PteGlu is drawn with thin bonds, as a reminder that it would not be present in the reaction of H_4PteGlu with the SHMT−Ser complex. No structure of a complex including serine and H_4PteGlu is available, but it is highly likely that the folate in such a complex occupies essentially the same position as 5-CHO-H_4PteGlu in the complexes that are pictured. Note that O_γ on C3 of serine is synperiplanar with respect to the PLP ring, and that the C2−C3 bond of serine is perpendicular to the plane of the ring. For the mechanism shown in Figure 1e, the sp^3 orbital on N5 of H_4PteGlu should be rotated 180° from the axis of the C2−C3 bond of serine, i.e., pointing approximately along the green arrow. For the mechanism shown in Figure 1d, the orbital should be 180° from the axis of the C3−O_γ bond of serine, approximately along the magenta arrow. This figure was drawn using Molscript (*32*) and Raster3D (*33*).

ficity at C3 suggest that abstraction of the C3 hydroxyl proton by a strong base (B_1 in Figure 1) is an unlikely first step in amino acid cleavage, with or without folate present.

An alternative to the two-step mechanism (Figure 1a,b) for the folate-dependent reaction is the proposed single-step nucleophilic displacement mechanism shown in Figure 1d; N5 of H_4PteGlu makes a direct attack on C3 of serine. This mechanism was proposed on the basis of the structure of the bsSHMT·Ser complex (*12*); it requires the serine hydroxyl to be synperiplanar to the aldimine nitrogen (as seen in the structure) and does not involve free formaldehyde. Hence, the stereochemical difficulties of the retroaldol mechanism are avoided. Additionally, the nucleophilic mechanism requires a proton donor (general acid) at the active site (H-bonded to the serine hydroxyl) to aid in the breaking of the O_γ−C3 bond, rather than a strong base. As described above, Glu75 is probably protonated and is well suited for this role. The direct displacement mechanism does not address the folate-independent cleavage of allothreonine and β-phenylserine, which is presumed to proceed via the retroaldol mechanism.

However, there is a serious problem with this nucleophilic mechanism. In the reverse reaction, the SHMT·Quin complex must accept a 1-C group from the iminium cation to form the covalent adduct. In the forward reaction, the iminium cation is formed via elimination of the serine hydroxyl as a water molecule. In the reverse reaction, this water would have to make an SN2 attack on C3 of serine, eliminating N5 of the covalent adduct. The SN2 substitution of a secondary amine with a weak base such as water would be very unfavorable. A second consideration is the geometry of the nucleophilic attack. For SN2 displacement, the attacking group should approach from the side opposite the leaving group; i.e., the sp^3 orbital of the tetrahedral N5 of H_4PteGlu should be positioned opposite the serine C3−O_γ bond. Examination of the structures of SHMT complexes with serine, and with 5-CHO−H_4PteGlu and glycine (Figure 7), reveals that N5 of H_4PteGlu is far from being in a good position to make an SN2 nucleophilic substitution of the serine hydroxyl.

A possible solution to the mechanistic problems described above is presented by a modified retroaldol mechanism based on the assumption that the critical factor in forming the transition state for cleavage of the C2−C3 bond of serine (and other substrates) is the highly electrophilic character of the PLP ring. The C2−C3 bond of serine is approximately orthogonal to the plane of the PLP ring in the bsSHMT structure, as first predicted by Dunathan (*35*). With this geometry, the strong electron withdrawing effect of PLP will polarize the C2−C3 bond, with positive charge accumulating on C3. An H-bond from Glu75, in its acid form, to O_γ will increase this charge even further. The polarized C2−C3 bond is easily broken. In the folate-independent cleavage (Figure 1a), it is not necessary for a strong base to form an alkoxide ion from the hydroxyl of the amino acid. Instead, the partial positive charge on C3 allows a weak base (e.g., water) to accept the proton from O_γ concomitantly with the breakage of the C2−C3 bond to form the aldehyde. Groups on C3 that can donate electrons by either inductive effects or resonance will lower the transition state energy, thus accounting for the substituent effects noted above. With serine, there are no electron-donating groups on C3 and the transition state energy for the folate-independent reaction will be higher than with allothreonine or phenylserine.

In view of the mechanistic problems described above, we propose the mechanism shown in Figure 1e for the serine and H_4PteGlu to glycine and CH_2-H_4PteGlu conversion. In this mechanism, the highly polarized C3 of serine is attacked by N5 of H_4PteGlu, cleaving the C2−C3 bond to generate N5-CHOH-H_4PteGlu (carbinolamine intermediate) and the quinonoid complex of glycine (SHMT·Quin). In this mechanism, the preferred direction for the nucleophilic attack by N5 on C3 of serine is opposite of the C3−C2 bond; i.e., the N5−C3−C2 angle should be close to 180°. As shown in Figure 7, N5 is much closer to being properly positioned for such an SN2 attack on C3 of serine (in which the glycine

anion is eliminated) than for the attack shown in Figure 1d (in which the serine hydroxyl is eliminated). Whether the reaction is concerted, as shown in Figure 1e, or stepwise, with breakage of the C2−C3 bond (creating a formaldehyde intermediate) preceding formation of the N5−C3 bond, awaits further study. We conclude, however, that this mechanism properly explains the role of Glu75 as an acid in both the retroaldol cleavage of all 3-hydroxy amino acids and the conversion of CH^+-H_4PteGlu to 5-CHO-H_4PteGlu.

REFERENCES

1. MacKenzie, R. E. (1984) Biogenesis and interconversion of substituted tetrahydrofolates, in *Folates and Pterins* (Blakely, R. L., and Benkovic, S. J., Eds.) Vol. 1, pp 255−306, Wiley, New York.
2. Schirch, L., and Gross, T. (1968) Serine transhydroxymethylase: identification as the threonine and allothreonine aldolases, *J. Biol. Chem. 243*, 5651−5655.
3. Ulevitch, R. J., and Kallen, R. G. (1977) Studies of the reactions of substituted D,L-erythro-β-phenylserines with lamb liver serine hydroxymethylase. Effects of substituents upon the dealdolization step, *Biochemistry 16*, 5342−5349.
4. Stover, P., and Schirch, V. (1990) Serine hydroxymethyltransferase catalyzes the hydrolysis of 5,10-methenyltetrahydrofolate to 5-formyltetrahydrofolate, *J. Biol. Chem. 265*, 14227−14233.
5. Stover, P., and Schirch, V. (1991) 5-Formyltetrahydrofolate polyglutamates are slow tight binding inhibitors of serine hydroxymethyltransferase, *J. Biol. Chem. 266*, 1543−1550.
6. Girgis, S., Suh, J. R., Jolivet, J., and Stover, P. J. (1997) 5-Formyltetrahydrofolate regulates homocysteine remethylation in human neuroblastoma, *J. Biol. Chem. 272*, 4729−4734.
7. Anguera, M. C., Rin Suh, J., Ghandour, H., Nasrallah, M., Selhub, J., and Stover, P. J. (2003) Methenyltetrahydrofolate synthetase regulates folate turnover and accumulation, *J. Biol. Chem. 278*, 29856−29862.
8. Renwick, S. B., Snell, K., and Baumann, U. (1998) The crystal structure of human cytosolic serine hydroxymethyltransferase: a target for cancer chemotherapy, *Structure 6*, 1105−1116.
9. Scarsdale, J. N., Radaev, S., Kazanina, G., Schirch, V., and Wright, H. T. (1999) Crystal structure of rabbit cytosolic serine hydroxymethyltransferase at 2.8 Å resolution: mechanistic implications, *Biochemistry 38*, 8347−8358.
10. Szebenyi, D. M. E., Liu, X., Kriksunov, I. A., Stover, P. J., and Thiel, D. J. (2000) Structure of a murine cytoplasmic serine hydroxymethyltransferase quinonoid ternary complex: evidence for asymmetric obligate dimers, *Biochemistry 39*, 13313−13323.
11. Scarsdale, J. N., Radaev, S., Kazanina, G., Schirch, V., and Wright, H. T. (2000) Crystal structure at 2.4 Å resolution of *E. coli* serine hydroxymethyltransferase in complex with glycine substrate and 5-formyl tetrahydrofolate, *J. Mol. Biol. 296*, 155−168.
12. Trivedi, V., Gupta, A., Jala, V. R., Sravanan, P., Rao, G. S. J., Rao, N. A., Savithri, H. S., and Subramanya, H. S. (2002) Crystal structure of binary and ternary complexes of serine hydroxymethyltransferase from *Bacillus stearothermophilus*: insights into the catalytic mechanism, *J. Biol. Chem. 277*, 17161−17169.
13. Stover, P., and Schirch, V. (1992) Enzymatic mechanism for the hydrolysis of 5,10-methenyltetrahydropteroylglutamate to 5-formyltetrahydropteroylglutamate by serine hydroxymethyltransferase, *Biochemistry 31*, 2155−2164.
14. Stover, P., and Schirch, V. (1992) Evidence for the accumulation of a stable intermediate in the nonenzymatic hydrolysis of 5,10-methenyltetrahydropteroylglutamate to 5-formyltetrahydropteroylglutamate, *Biochemistry 31*, 2148−2155.
15. Matthews, R. B., and Drummond, J. T. (1990) Providing one-carbon units for biological methylations: mechanistic studies on serine hydroxymethyltransferase, methylenetetrahydrofolate reductase, and methyltetrahydrofolate-homocysteine methyltransferase, *Chem. Rev. 90*, 1275−1290.
16. Krishna Rao, J. V., Prakash, V., Appaji Rao, N., and Savithri, H. S. (2000) The role of Glu74 and Tyr82 in the reaction catalyzed by sheep liver cytosolic serine hydroxymethyltransferase, *Eur. J. Biochem. 267*, 5967−5976.
17. Iurescia, S., Condò, I., Angelaccio, S., Delle Fratte, S., and Bossa, F. (1996) Site-directed mutagenesis techniques in the study of *Escherichia coli* serine hydroxymethyltransferase, *Protein Expression Purif. 7*, 323−328.
18. Schirch, V., Shostak, K., Zamora, M., and Gautam-Basak, M. (1991) The origin of reaction specificity in serine hydroxymethyltransferase, *J. Biol. Chem. 266*, 759−764.
19. Schirch, L., and Ropp, M. (1967) Serine transhydroxymethylase, affinity of tetrahydrofolate compounds for the enzyme and enzyme-glycine complex, *Biochemistry 6*, 253−257.
20. Stover, P., Zamora, M., Shostak, K., Gautam-Basak, M., and Schirch, V. (1992) *Escherichia coli* serine hydroxymethyltransferase: the role of histidine 228 in determining reaction specificity, *J. Biol. Chem. 267*, 17679−17687.
21. Leslie, A. G. W. (1992) Recent changes to the MOSFLM package for processing film and image plate data, *Joint CCP4 and ESF-EAMCB Newsletter on Protein Crystallography*, No. 26.
22. Evans, P. R. (1993) Data reduction, *Proceedings of the CCP4 Study Weekend on Data Collection and Processing*, pp 114−122, SRC Daresbury Laboratory, Warrington, U.K.
23. Nielsen, C., Arvai, A., Szebenyi, D. M. E., Deacon, A., Thiel, D. J., Bolotovsky, R., Van Zandt, K. C., and Rossmann, M. (1998) DPS: a data processing system for oscillation method data from a 2 × 2 mosaic CCD detector, ACA Annual Meeting July 18−23, 1998, Arlington, VA, Abstract 11.06.06.
24. Brunger, A. T., Adams, P. D., Clore, G. M., DeLano, W. L., Gros, P., Grosse-Kunstleve, R. W., Jiang, J.-S., Kuszewsi, J., Nilges, N., Pannu, N. S., Read, R. J., Rice, L. M., Simonson, T., and Warren, G. L. (1998) Crystallography & NMR system: a new software suite for macromolecular structure determination, *Acta Crystallogr. D54*, 905−921.
25. Jones, T. A., Zou, J. Y., Cowan, S. W., and Kjeldgaard, M. (1991) Improved methods for building protein models in electron density maps and the location of errors in these models, *Acta Crystallogr. A47*, 110−119.
26. Fu, T.-F., Scarsdale, J. N., Kazanina, G., Schirch, V., and Wright, H. T. (2003) Location of the pteroylpolyglutamate-binding site on rabbit cytosolic serine hydroxymethyltransferase, *J. Biol. Chem. 278*, 2645.
27. Berman, H. M., Westbrook, J., Feng, Z., Gilliland, G., Bhat, T. N., Weissig, H., Shindyalov, I. N., and Bourne, P. E. (2000) The protein data bank, *Nucleic Acids Res. 28*, 235−242.
28. Schirch, L. (1975) Serine transhydroxymethylase: relaxation and transient kinetic study of the formation and interconversion of the enzyme-glycine complexes, *J. Biol. Chem. 250*, 1939−1945.
29. Chen, M. S., and Schirch, L. (1973) Serine transhydroxymethylase: a kinetic study of the synthesis of serine in the absence of tetrahydrofolate, *J. Biol. Chem. 248*, 3631−3635.
30. Chen, M. S., and Schirch, L. (1973) Serine transhydroxymethylase: studies on the role of tetrahydrofolate, *J. Biol. Chem. 248*, 7979−798.
31. Schirch, L., and Mason, M. (1963) Serine transhydroxymethylase: a study of the properties of a homogeneous enzyme preparation and of the nature of its interaction with substrates and pyridoxal 5′-phosphate, *J. Biol. Chem. 238*, 1032−1037.
32. Kraulis, P. J. (1991) A program to produce both detailed and schematic plots of protein structures, *J. Appl. Crystallogr. 24*, 946−950.
33. Merritt, E. A., and Bacon, D. J. (1997) Raster3D: photorealistic molecular graphics, *Methods Enzymol. 277*, 505−524.
34. Schirch, L., and Diller, A. (1971) Serine transhydroxymethylase: affinity of the active site for substrates, substrate analogues, and anions, *J. Biol. Chem. 246*, 3961−3966.
35. Dunathan, H. C. (1966) Conformation and reaction specificity in pyridoxal phosphate enzymes, *Proc. Natl. Acad. Sci. U.S.A. 55*, 712−716.
36. Tatum, C. M., Jr., Benkovic, P. A., Benkovic, S. J., Potts, R., Schliecher, E., and Floss, H. G. (1977) Stereochemistry of methylene transfer involving 5,10-methylenetetrahydrofolate, *Biochemistry 16*, 1093−1102.
37. Vanoni, M. A., Lee, S., Floss, H. G., and Matthews, R. G. (1990) Stereochemistry of reduction of methylenetetrahydrofolate to methyltetrahydrofolate catalyzed by pig liver methylenetetrahydrofolate reductase, *J. Am. Chem. Soc. 112*, 3987−3992.
38. Webb, H. K., and Matthews, R. G. (1995) 4-Chlorothreonine is substrate, mechanistic probe, and mechanism-based inactivator of

serine hydroxymethyltransferase, *J. Biol. Chem. 270*, 17204−17209.

39. Quashnock, J. M., Chelbowski, J. F., Martinez-Carrion, M., and Schirch, L. (1983) Serine hydroxymethyltransferase: ^{31}P nuclear magnetic resonance study of the enzyme-bound pyridoxal 5′-phosphate, *J. Biol. Chem. 258*, 503−507.
40. Schirch, L., and Schnackerz, K. D. (1978) Activation of aposerine transhydroxymethylase by pyridoxal-5′-phosphate monomethyl ester, *Biochem. Biophys. Res. Commun. 85*, 99−106.
41. Hopkins, S., and Schirch, V. (1986) Properties of a serine hydroxymethyltransferase in which an active site histidine has been changed to an asparagine by site-directed mutagenesis, *J. Biol. Chem. 261*, 3363−3369.
42. Jagath, J. R., Sharma, B., Rao, N. A., and Savithri, H. S. (1997) The role of His-134, -147, and -150 residues in subunit assembly, cofactor binding, and catalysis of sheep liver cytosolic serine hydroxymethyltransferase, *J. Biol. Chem. 272*, 24355−24362.

BI049791Y